Phys. Status Solidi A **212,** No. 2, 239–244 (2015) / **DOI** 10.1002/pssa.201400158

physica status solidi a
www.pss-a.com
applications and materials science

Control of resistive switching in AM_4Q_8 narrow gap Mott insulators: A first step towards neuromorphic applications

Julien Tranchant[*,1], Etienne Janod[1], Benoît Corraze[1], Pablo Stoliar[1,2,3], Marcelo Rozenberg[4], Marie-Paule Besland[1], and Laurent Cario[,1]**

[1] Institut des Matériaux Jean Rouxel, Université de Nantes, CNRS, 2 rue de la Houssinière, BP 32229, 44322 Nantes Cedex 3, France
[2] CIC nanoGUNE, 20018 Donostia – San Sebastian, Basque Country, Spain
[3] ECyT, Universidad Nacional de San Martín, Campus Miguelete 1650 San Martín, Argentina
[4] Laboratoire de Physique des Solides, CNRS UMR 8502, Université Paris Sud, Bât. 510, 91405 Orsay, France

Received 23 June 2014, accepted 23 July 2014
Published online 13 November 2014

Keywords memristor, Mott insulator, RRAM, resistive switching

[*] Corresponding author: e-mail julien.tranchant@cnrs-imn.fr, Phone: +33 240 373 937, Fax: +33 240 373 991
[**] e-mail laurent.cario@cnrs-imn.fr, Phone: +33 240 373 988, Fax: +33 240 373 991

The AM_4Q_8 family of chalcogenide Mott insulator compounds exhibit an electric pulse induced resistive switching that could be used in data storage applications as Mott memories. Depending on the applied electric field, this transition is either volatile or non-volatile. This study demonstrates that the theory established for the volatile transition can be used to understand the non-volatile transition. It leads to propose a simple model for the SET and RESET transitions. In addition, we show that the alternation of short high voltage multi-pulses with long low voltage single pulses enables to control the non-volatile resistive switching and to achieve multi-level switching. This memristive property opens the way to the use in neuromorphic applications of this new type of resistive switching inherent to Mott insulators.

1 Introduction Flash technology has been leading the field of non-volatile memories for more than 10 years. In relation with the constant increase of integration density, this technology will soon reach its physical limitations. For this reason, new classes of materials have raised as candidates for non-volatile data storage, amongst which resistive random access memories (ReRAM) are considered as very promising [1–3]. In the ReRAM technology, the binary logic is based on two different resistance levels of the material, i.e. a low resistance state (LRS) and a high resistance state (HRS). Applying electric pulses enables to switch back and forth between both resistance states. But, recently, tuneable multilevel switching was also demonstrated on ReRAM materials. This discovery offers new insights in the field of neurocomputing [4]. Indeed, such memristive behaviour offers a very simple solution to implement artificial synapses, whose conductance state (i.e. synaptic weight), is defined by the history of pulses that have passed through it [5]. Therefore, many researches aim at replacing complex sets of components needed to reproduce the behaviour of biological synapses by a very simple ReRAM metal-insulator-metal (MIM) structure.

So far, resistive switching mechanisms are ascribed to various physical phenomena, including electro-chemical and thermo-chemical effects leading to various types of ReRAM [1, 2]. The corresponding taxonomy is yearly published in the International Technology Roadmap for Semiconductors (ITRS) [6]. In the last editions of ITRS, a new class of 'emerging research memory devices', mentioned as 'Mott memories', is reported. Chalcogenide Mott insulators AM_4Q_8 (A = Ga, Ge; M = V, Nb, Ta; Q = S, Se) belong to this class of Mott memories. They store binary data using a new mechanism of resistive switching based on the Mott metal–insulator-transition (MIT). Application of electric pulses in these compounds induces an electric-field driven resistive switching (RS) which originates from an avalanche phenomenon [7]. Depending on the strength of the applied electric field the RS is either volatile or non-volatile [8, 9].

The volatile RS observed above a threshold electric field of a few kV/cm is highly reproducible. It has been extensively studied, leading to a fine understanding of the physical mechanisms involved in this phenomenon. A simple model shows that this volatile RS results from the breakdown of the Mott insulating state at the nanoscale, which triggers the creation of a conducting filamentary path by accumulation of correlated metallic sites [10]. On the other hand, the non-volatile RS observed much above the threshold electric field remains far less understood, even if thin film processability has enabled to demonstrate very promising memory performances [11–14]. A better understanding of this transition is therefore required to take its control and open new perspectives for data storage or neuromorphic applications. Here, we show that the model established for the volatile RS can be used as a starting point to understand the non-volatile transition. Our experiments show that the SET transition (i.e. from HRS to LRS) arises from the same process of accumulation of correlated metallic sites as observed for the volatile transition. On the other hand, the RESET transition (i.e. from LRS back to HRS) can be achieved by a thermal relaxation of these metallic sites. Alternating short high voltage multi-pulses with long low voltage single pulses allows therefore to achieve a better control of the non-volatile transition and to reach multilevel switching. This memristive behaviour is a first step towards neuromorphic applications based on Mott insulators.

2 Experimental details The experimental set-up used for the application of pulses is displayed in Fig. 1a. It consists of a pulse generator (Agilent 8114A) placed in series with a load resistor and home-synthesised GaV_4S_8 or $GaTa_4Se_8$ crystals. The electrical connection to the freshly cleaved crystal is ensured by two gold wires through carbon paste. The preparation of these samples is described elsewhere [8]. Between the application of pulses, the sample resistance is measured at low bias (10 mV) by a Keithley 6430 source-measure unit via a parallel circuit.

3 Results and discussion

3.1 Model for volatile resistive switching The volatile resistive switching observed in the AM_4Q_8 compounds is very reproducible and originates from an avalanche breakdown mechanism, which induces the Mott MIT, namely the collapse of the Mott insulating (MI) state into a correlated metallic (CM) state. This transition between both states can be modelled [10] thanks to the energy landscape presented in Fig. 2a, in which the CM state has a higher energy E_{CM} than the MI state, since the compounds are normally insulating. In order to reflect the metastable character of the CM state, an energy barrier E_B separates it from the MI state.

The application of an electric field increases the energy level of the MI state, and thus lowers the difference in energy between both states. This energy landscape is implemented in each cell of the resistor network shown in Fig. 2b. Each cell is either in MI or in CM state, and its resistance is either in high or low resistance state R_{MI} or R_{CM}. Initially all cells are in MI state. In order to reproduce the experimental set-up described in Fig. 1a, the resistor network is connected in series with a

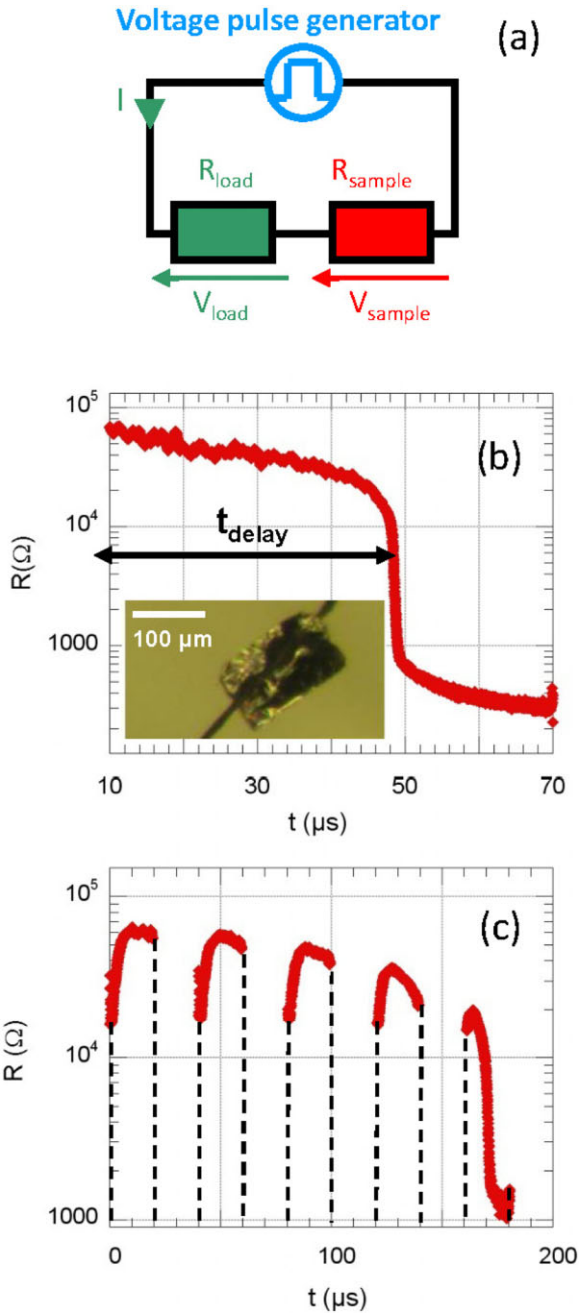

Figure 1 (a) Experimental set-up used for the application of pulses to the sample, which is placed in series with a load resistance and a voltage pulse generator. (b) Volatile resistive switch observed on a $GaTa_4Se_8$ crystal (see inset) at 70 K, after a delay time $t_{delay} = 48$ µs, during the application of a 70 µs/35 V pulse. (c) Evidence of pulse accumulation effect on the volatile resistive switch in the $GaTa_4Se_8$ crystal shown in (b), when five pulses of 20 µs/35 V separated by 20 µs off periods are applied.

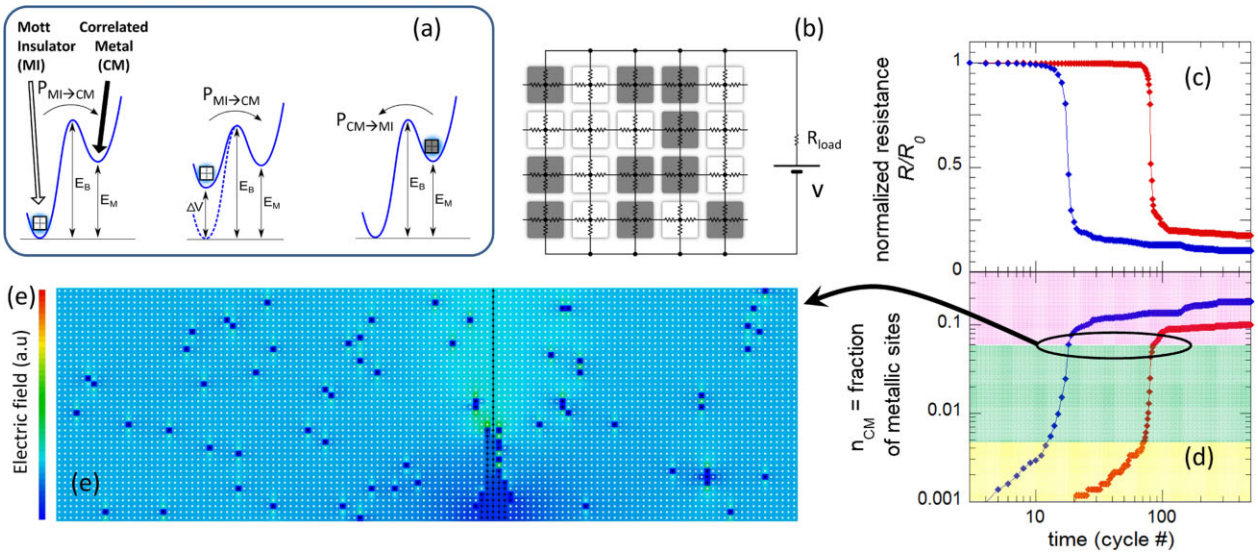

Figure 2 (a) Energy landscape model used to simulate the Mott MIT driven by an external electric field. This landscape is applied to every cell of the resistor network (b), where grey and white dots represent respectively cells in the MI and CM (transited) states. (c) Resulting simulated evolution of normalised resistance R/R_0. The applied voltage is higher for the blue curve than for the red one. (d) Associated increasing fraction of metallic sites in the resistor network. The yellow, green and pink areas correspond respectively to the increase of metallic cells before, during and after the creation of the filamentary percolating path. (e) Representation of the resistor network and associated electric field, just after the creation of this filament.

load resistance to a voltage power supply (see Fig. 2b). In this model the MI → CM transition rate of each cell is given by

$$P_{\mathrm{MI}\rightarrow\mathrm{CM}} = \nu e^{-\frac{E_B - q|\Delta V|}{kT}}, \quad (1)$$

where the constant ν is an attempt rate, q is the charge, T is the temperature and ΔV is the local voltage drop for the considered cell. Conversely, the CM → MI transition rate is given by

$$P_{\mathrm{CM}\rightarrow\mathrm{MI}} = \nu e^{-\frac{E_B - E_M}{kT}}. \quad (2)$$

This model suggests then that the MI → CM transition is mainly dependent on the electric field, while the CM → MI transition is the thermally activated relaxation from a metastable state.

This model predicts that the metallic sites accumulate with time (yellow region in Fig. 2d) in the material until a critical density of CM regions sets off an avalanche-like process that ends in the formation of a conductive path connecting the electrodes (green region in Fig. 2d). A typical filament is presented in Fig. 2e, just after its creation, which leads to a resistive switching. The rate of accumulation of metallic sites accelerates when the applied electric field increases. As a consequence for higher voltage the slope for the creation of metallic sites is steeper (yellow region in Fig. 2d) and the time for the creation of the filament is shorter (green region in Fig. 2d). The model reproduces therefore the experimental phenomenology of the RS. Especially the delay time after which the transition occurs shows a reciprocal variation versus the applied voltage (compare theoretical results displayed in Fig. 2c with experimental results displayed in Fig. 1b) [7, 10].

On the other hand the model predicts that after the pulse, when the voltage is released, correlated metallic sites can go back to the insulating state owing to a thermal relaxation process [7, 10]. The effect of accumulation and relaxation of correlated metallic states can be directly observed when a train of pulses is applied to the material. Figure 1c displays the evolution of resistance in a GaV_4S_8 crystal during the application of 20 μs/35 V pulses separated by 20 μs. Under this voltage, the delay time after which the volatile transition occurs is 48 μs (see Fig. 1b). This means that assuming a fast relaxation of the CM sites (<1 μs) no transition should occur, while without relaxation a transition should be observed for the third pulse. Figure 1c shows that none of these situations occurs but that the volatile RS is observed during the 5th pulse. This volatile RS demonstrates therefore the accumulation of CM sites during the pulses and the incomplete relaxation of these sites between the pulses [7, 10].

3.2 Control of the non-volatile resistive switching (SET transition) While our previous works are able to describe most of the mechanisms involved in the volatile RS, the NV transition remains misunderstood and hardly predictable. Nevertheless, our studies reveal that increasing the electric field applied to the material to a few E_{th} can trigger a NV RS [8, 9]. As shown in Fig. 2, the increase of the electric field in a given time results in

increasing the number of metallic sites inside the material. Yet the model displayed in Fig. 2 suggests another strategy to increase the number of metallic sites, which consists in increasing the application time of a given electric field. Indeed, even after the creation of the percolating filamentary path, the number of sites still goes on increasing, as shown in Fig. 2d (pink region). However, the application of long pulses at a high electric field may destroy the material by Joule heating. Moreover, the model suggests that the CM → MI transition is thermally activated. Applying long pulses of high amplitude could thus result in a competition between creation and relaxation of metallic sites. In order to increase the application time of the electric field while limiting the thermal effects by Joule heating, a strategy can then consist in applying trains of pulses, which have proven to enable the accumulation of metallic sites inside the material [10]. In addition a load resistance of sufficient value should limit the current and therefore restrict thermal effects.

Thereby, as displayed in Fig. 3, the application of a 120 V/30 μs pulse to a pristine GaV_4S_8 crystal placed in series with a 5 kΩ load resistance triggers a volatile transition. Indeed, a RS occurs during the pulse but the resistance state after the application of the pulse goes back to the pristine value. However, if the same pulse is applied seven times, with a period of 200 μs, this transition becomes non-volatile, since the resistance has changed from 42.4 to 1.6 kΩ after the train of pulses. It has to be noticed that the transition observed in the first pulse of the train is perfectly similar to the one observed when applying only one 120 V/30 μs pulse. Nevertheless, the time evolution of the resistance in the subsequent pulses is definitively different. Between two pulses the resistance does not go back to a HRS. This is a clear illustration of an accumulation of CM sites with incomplete relaxation between the pulses as already described in Fig. 1c. However, while the experiment depicted in Fig. 1c leads to a volatile transition, here after the 7th pulse the resistance remains in a LRS, i.e. the transition becomes non volatile. This experiment therefore suggests that the accumulation of CM sites has triggered the stabilisation of the LRS. It shows therefore that the NV transition is directly linked to the accumulation of metallic sites inside the material. This is consistent with the results of the model presented in Fig. 2. According to the model, the increase of electric field provokes the growth of the filament in diameter while it leads to a non-volatile transition in our experiments [10]. Based on these remarks, the NV stabilisation of the conductive filamentary path is then fully consistent with the accumulation of metallic sites inside the material, inducing the growth of the filament, as successive pulses are applied or the electric field is raised. This is in agreement with classical nucleation growth mechanisms based on the assumption that growth takes place by the generation and subsequent enlargement of nuclei that become stable only above a critical size [15].

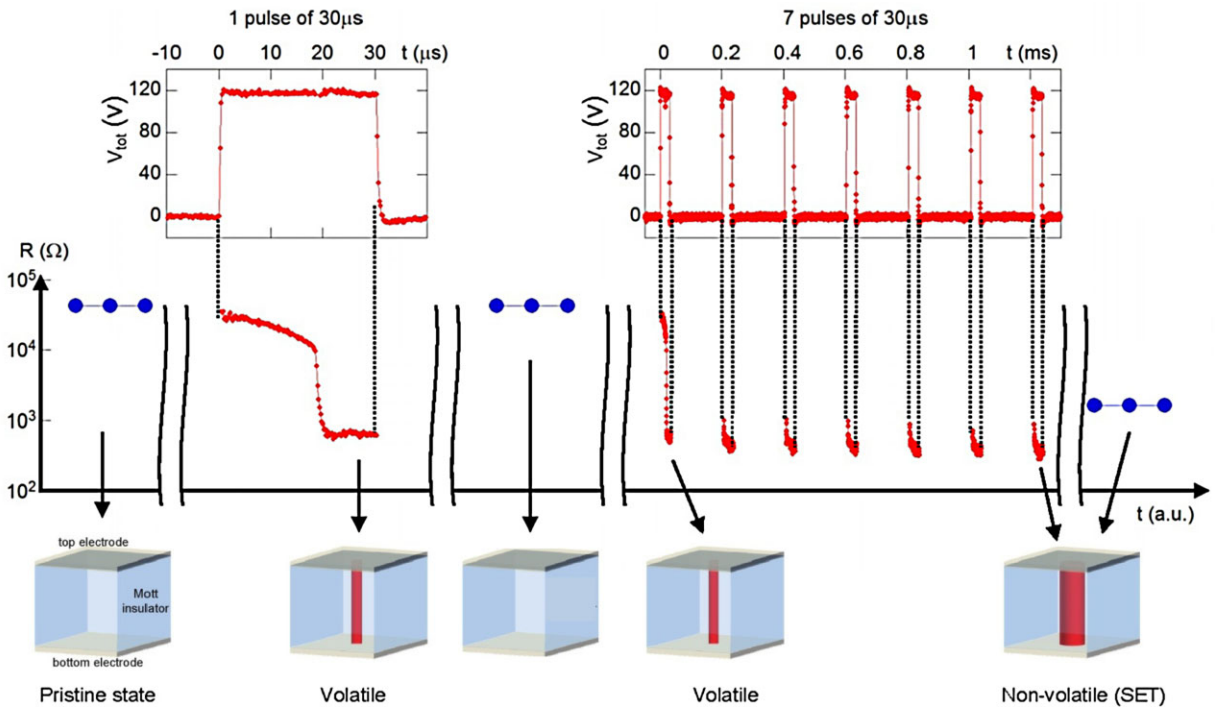

Figure 3 Evolution of resistance in a GaV_4S_8 crystal, before, during and after the application of one pulse of 30 μs/120 V, and then a train of 7 pulses of 30 μs/120 V separated by 170 μs off period. The resistance between pulses (blue circles) is measured at low bias. The additional sketches illustrate the evolution of the conductive filamentary path through the successive application of pulses.

3.3 Control of the RESET transition In order to control the NV RS towards data storage or neuromorphic applications, the inverse transition from LRS to HRS, namely the RESET transition has also to be monitored. The energy landscape model suggests that the CM → MI transition is thermally activated. Following this hypothesis, the Joule self-heating of the filament might induce a thermal relaxation of the CM states and dissolve the conductive percolating path. Here again, in order to avoid the creation of metallic sites that would compete with their relaxation, long pulses with low-electric field have to be preferred. Moreover, a low load resistance might enable a high current to flow through the filament, thus maximizing the Joule heating.

Figure 4 illustrates the use of this strategy. Several 10–20 V/0.5 ms pulses were applied to the experimental set-up, with a load resistance of 100 Ω. No resistance variation was observed. However, if the pulse length is increased to 2 ms, with 12 V voltage, the resistance rises to 36.7 kΩ. This value is very close to the pristine state (42.4 kΩ), which suggests that the filament has been dissolved almost entirely. This impact of the pulse time increase is clearly in agreement with a thermal mechanism for the RESET transition.

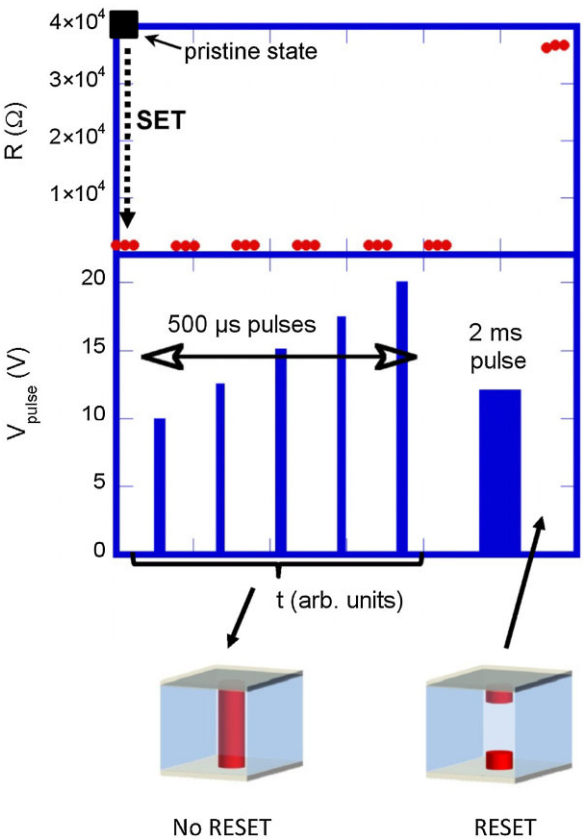

Figure 4 Effect of pulse duration on the RESET transition in a GaV_4S_8 crystal. 500 µs pulses in the 10–20 V range induce no resistance modification, while a 2 ms/12 V pulse induces the RESET transition. The sketches illustrate the associated filament evolution.

3.4 Towards multilevel switching The better understanding of SET and RESET transitions is a prerequisite step to elaborate a strategy to tune the non-volatile RS. Figure 5 shows, as an example that the alternation of high voltage short multi-pulses with low voltage long single pulses enables to control RS cycles between a HRS and a LRS. It has to be noticed that the voltage needed to induce the HRS → LRS transition, from the second cycle, is lower than in the pristine state, which is fully consistent with the partial dissolution of the conductive filamentary path.

The partial destruction/reformation of the filamentary conducting path may give the opportunity to reach multilevel switching. The last RESET observed in Fig. 5 is obtained with a 5 kΩ load resistance, which is limiting drastically the current compared to the 100 Ω load resistance used for the previous RESET. For this last RESET, the resistance does not come back to the value close to the pristine value but reaches an intermediate value between the LRS and the HRS (i.e. 19 kΩ). This result is in perfect agreement with the model proposed for the RESET transition, since the higher load resistance used induces lower current and voltage through the sample, and then lower power dissipation. The self Joule heating of the filamentary path is thus decreased and the filament dissolution is limited compared to previous cycles.

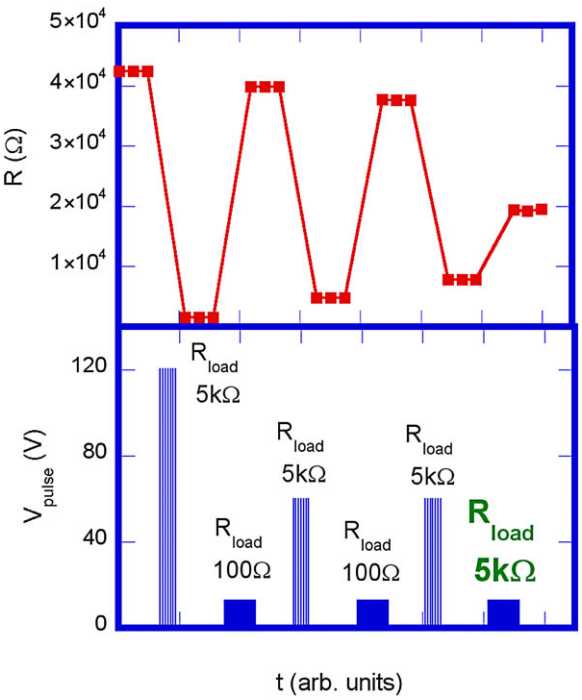

Figure 5 Resistance switching cycles obtained in a GaV_4S_8 crystal submitted to an alternation of multi-pulses (seven pulses of 30 µs separated by 170 µs off period) and single pulses (2 ms). Load resistances of 5 kΩ and 100 Ω are respectively used for the application of multi-pulses and single pulses, except for the last single pulse. In this latter case, a 5 kΩ load resistance induces an intermediate resistance state between LRS and HRS.

4 Conclusion We have performed a comprehensive set of experiments to improve knowledge of the non-volatile resistive switching in Mott insulators. Our experiments suggest that the SET transition arises from the growth of conducting filamentary paths and their stabilisation above a critical size. On the other hand, our experiments suggest that the RESET transition is due to the thermal relaxation from a metastable state, therefore, the conductive path may be destroyed by the effect of self Joule heating. This better understanding of the RS in the Mott insulators AM_4Q_8 enables the control of multi-level non-volatile resistance states. The proposed strategy is simple and consists in alternating multi-pulses for the SET with long single pulses for the RESET with varying duration and voltages. This is a first step to the mastership of memristive behaviour that could open the way towards application of these Mott insulators as artificial synapses in neuromorphic systems.

Acknowledgements The authors acknowledge CNano Nord-Ouest, Région Pays-de-la-Loire, CNRS and Ramon y Cajal (RYC-2012-01031) program for funding. The French Agence Nationale de la Recherche is also deeply thanked for its support on this work through the funding of the 'NV-CER' (ANR-05-JCJC-0123-01), 'NanoMott' (ANR-09-Blan-0154-01) and 'Mott-RAM' (ANR-2011-EMMA-016-01) projects.

References

[1] A. Sawa, Mater. Today **11**, 28 (2008).
[2] R. Waser and M. Aono, Nature Mater. **6**, 833 (2007).
[3] Y. V. Pershin and M. Di Ventra, Adv. Phys. **60**, 145 (2011).
[4] C. Mead, Proc. IEEE **78**, 1629 (1990).
[5] C. Zamarreño-Ramos, L. A. Camuñas-Mesa, J. A. Pérez-Carrasco, T. Masquelier, T. Serrano-Gotarredona, and B. Linares-Barranco, Front. Neurosci. **5**(26), 1 (2011).
[6] International Technology Roadmap for Semiconductors - Emerging research devices, to be found under http://www.itrs.net/Links/2013ITRS/2013Chapters/2013ERD.pdf.
[7] V. Guiot, L. Cario, E. Janod, B. Corraze, V. Ta Phuoc, M. Rozenberg, P. Stoliar, T. Cren, and D. Roditchev, Nature Commun. **4**, 1722 (2013).
[8] C. Vaju, L. Cario, B. Corraze, E. Janod, V. Dubost, T. Cren, D. Roditchev, D. Braithwaite, and O. Chauvet, Adv. Mater. **20**, 2760 (2008).
[9] L. Cario, C. Vaju, B. Corraze, V. Guiot, and E. Janod, Adv. Mater. **22**, 5193 (2010).
[10] P. Stoliar, L. Cario, E. Janod, B. Corraze, C. Guillot-Deudon, S. Salmon-Bourmand, V. Guiot, J. Tranchant, and M. Rozenberg, Adv. Mater. **25**, 3222 (2013).
[11] J. Tranchant, E. Janod, L. Cario, B. Corraze, E. Souchier, J.-L. Leclercq, P. Cremillieu, P. Moreau, and M.-P. Besland, Thin Solid Films **533**, 61 (2013).
[12] J. Tranchant, A. Pellaroque, E. Janod, B. Angleraud, B. Corraze, L. Cario, and M.-P. Besland, J. Phys. D: Appl. Phys. **47**, 65309 (2014).
[13] E. Souchier, L. Cario, B. Corraze, P. Moreau, P. Mazoyer, C. Estournes, R. Retoux, E. Janod, and M. P. Besland, Phys. Status Solidi RRL **5**, 53 (2011).
[14] E. Souchier, M.-P. Besland, J. Tranchant, B. Corraze, P. Moreau, R. Retoux, C. Estournès, P. Mazoyer, L. Cario, and E. Janod, Thin Solid Films **533**, 54 (2013).
[15] C. M. Pina, A. Putnis, and J. M. Astilleros, Chem. Geol. **204**, 145 (2004).

